Proceedings of the 21st ICSMGE, Vienna, Austria, 14 – 19 June 2026. Pistrol, Adam & Schweiger (eds.)
Published by: ÖGG, Austrian Society for Geomechanics, Salzburg, Austria, ISBN 978-3-9503898-4-5
https://doi.org/10.53243/ICSMGE2026-437

Advanced numerical study on strain history and shear strain effects in Reliquefaction resistance

Rafael Iglesias
Geotechnics Section, Arcadis, Santiago, Chile, rafael.iglesias@arcadis.com

Stavroula Kontoe
Department of Civil Engineering, University of Patras, Patras, Greece, skontoe@upatras.gr; Department of Civil and Environmental Engineering, Imperial College London, United Kingdom

Julia Katharina Möller
Wood Thilsted, London, United Kingdom, jkm@woodthilsted.com; Department of Civil and Environmental Engineering, Imperial College London, United Kingdom

ABSTRACT: It is commonly assumed that soils increase their resistance to liquefaction following an initial liquefaction event due to densification during reconsolidation. However, emerging evidence (Finn et al. 1970; Seed et al. 1977; Ishihara & Okada 1978) suggests that strain history, anisotropy (Yamada et al. 2010; Nemat-nasser & Takahashi 1984), and fabric changes (Nemat-nasser & Takahashi 1984; Nemat-nasser & Tobita 1982) can have a more significant impact than density on post-liquefaction resistance. This study examines the effect of strain history on reliquefaction resistance of Ottawa F-65 sand through numerical modelling using the PM4Sand constitutive model. Finite element simulations are conducted to replicate cyclic direct simple shear (CDSS) tests, with a focus on evaluating the influence of strain history on reliquefaction resistance. The results demonstrate that there is a shear strain threshold beyond which reliquefaction resistance decreases, as suggested initially by Finn et al. (1970). The study highlights the value of advanced constitutive models in understanding reliquefaction mechanisms and improving seismic hazard mitigation strategies.

KEYWORDS: Liquefaction, Reliquefaction, PM4Sand.

1 INTRODUCTION

Liquefaction remains one of the most critical geotechnical hazards associated with seismic events. While significant research has been focused on understanding liquefaction triggering, the phenomenon of reliquefaction has gained increasing attention in recent years due to its implications for the seismic performance of structures (Yamada et al. 2010; Parra Bastidas, 2016; Yasuda & Tohno 1988). Reliquefaction refers to the occurrence of liquefaction in a previously liquefied soil, after a reconsolidation phase has taken place. For the purposes of this study, the term "liquefaction" will be used to refer to a state where a single amplitude shear strain of 3.0 % has been reached due to a significant rise in pore water pressure.

This paper presents a numerical study focused on the influence of maximum shear strain experienced during an initial liquefaction event on the subsequent resistance to reliquefaction.

2 BACKGROUND ON RELIQUEFACTION

Reliquefaction has been documented in several seismic events. In Japan, the 1983 Nihonkai-Chubu earthquake provides evidence of reliquefaction at 11 sites, with some locations experiencing liquefaction up to five times during 1964 to 1983, as indicated by Yasuda & Tohno (1988). In New Zealand, earthquakes in Christchurch between September 2010 and December 2011 (Mw 5.3 to 7.1) also showed numerous reliquefaction cases (Cubrinovski et al. 2012; Van Ballegooy 2014). In Chile, studies following the 2010 Maule Earthquake (Mw=8.8) suggest that sites that liquefied during the 1960 Valdivia earthquake (Mw=9.5) were still prone to liquefaction and did so again in 2010, as indicated by Verdugo & González (2015).

Among the earliest studies on reliquefaction, Finn et al. (1970) performed both cyclic undrained triaxial tests and undrained cyclic direct simple shear tests on Ottawa Sand. Their findings revealed that reliquefaction resistance significantly decreased on both cyclic triaxial and cyclic direct simple shear tests where large strains were developed. On the other hand, their results suggested that for cyclic events with small strains and low excess pore water pressures, which do not reach a state of full liquefaction, the resistance to reliquefaction significantly increases, as the elimination of local instabilities allows for a better interlocking of particles. They postulated the existence of a threshold shear strain value beyond which reliquefaction resistance decreases if that threshold was exceeded during a previous liquefaction event.

Subsequently, Yamada et al. (2010) concluded that during liquefaction, anisotropy is developed and remains even after liquefaction, which can significantly decrease the resistance to reliquefaction for certain shaking directions.

3 METHODOLOGY

This study builds upon the numerical modeling work by Parra Bastidas (2016), in which the PM4Sand (Boulanger, & Ziotopoulou, 2013) constitutive model was calibrated to simulate 16 consecutive cyclic direct simple shear tests with Ottawa Sand samples. Table 1 summarizes the main grain size characteristics of Ottawa F-65 sand:

Table 1. Ottawa F-65 sand grain size characteristics.

D_{60} [mm]	D_{10} [mm]	D_{30} [mm]	C_u	C_c	Fines content [%]	USCS
0.22	0.13	0.17	1.61	0.96	0.20	SP

The calibration was validated through comparison with experimental results, and the same set of model parameters used in calibration No. 2 by Parra Bastidas (2016) was adopted for this study. In general, calibration N°2 better reproduces the soil behaviour of samples with lower relative densities. Table 2 presents the model parameters considered.

Table 2. Calibration parameters adopted from Parra Bastidas (2016).

Type of parameter	Parameter	Value
Primary	DR	between 30% and 74%
Primary	G_o	Calculated from DR.
Primary	h_{po}	0.32 for loose samples
Primary	h_{po}	0.016 for dense samples
Secondary	e_{max}	0.833
Secondary	e_{min}	0.507
Secondary	φ_{cv}	30°
Secondary	R	1.00
Secondary	Q	10 (default PM4Sand value)
Secondary	V	0.3 (default PM4Sand value)
Secondary	n_b	0.25
Secondary	n_d	0.1 (default PM4Sand value)
Secondary	h_o	Default PM4Sand expression.
Secondary	A_{do}	Default value, based on Seed et al. (1977)
Secondary	z_{max}	Default PM4Sand expression.
Secondary	C_z	250 (Default PM4Sand value)
Secondary	Cε	Default PM4Sand expression.
Secondary	C_{DG}	2.0 (default PM4Sand value)
Secondary	C_α	Default PM4Sand expression.
Secondary	M	0.01(default PM4Sand value)

44 single-element simulations of cyclic direct simple shear tests (CDSS) were performed, each considering different relative density and cyclic stress ratio (CSR) values. Each simulation included two consecutive undrained (constant height condition) CDSS tests. All simulations began with an initial vertical effective stress of σ_v'=100 kPa, and a different initial relative density was adopted at the start of each simulation. After the 1st undrained CDSS test was simulated, the sample was re-centered, followed by a reconsolidation phase. Finally, the 2nd undrained CDSS test was simulated to evaluate the effect that the maximum shear strain (γ_{max}) reached during the 1st cyclic loading phase has on the liquefaction resistance during the 2nd cyclic loading phase.

The simulations were conducted using the PLAXIS 2D (version 22.01.00.452.) software and were organized into four Groups (A, B, C, and D), based on the maximum shear strain (γ_{max}) developed during the first cyclic loading event. Each group considers 11 single element simulations, with each simulation consisting of two consecutive cyclic simple shear tests. In Group A, γ_{max} was approximately 3.0% during the first loading cycle. For Group B, γ_{max} was close to 1.0%. In Group C, γ_{max} reached approximately 0.2% and in Group D, γ_{max} was about 0.1%.

Tests in each Group were conducted at relative densities ranging from 30% to 74%, with CSR values between 0.12 (for looser samples) and 0.40 (for denser samples).

Table 3 indicates the applied cyclic stress ratio and the relative density considered in each simulation. It is important to highlight that, as the relative density increases, the CSR applied was also increased in order to facilitate the liquefaction triggering in denser samples.

Table 3. Relative density and CSR considered in each simulation.

Type of density	Initial Relative density [%]	CSR
Loose	30	0.12
Loose	35	0.12
Loose	41	0.12
Dense	72	0.25
Dense	74	0.40

Figure 1 presents the results of 1 of the 44 simulations conducted. In this case, γ_{max} reached around 3% during the first cyclic test. During this initial cyclic loading, the element experienced 7 cycles before liquefying. Following this initial cyclic loading phase, a reconsolidation process was performed, during which the sample underwent an increase in relative density. In the 2nd cyclic loading test, excess pore water pressure developed extremely quickly, resulting in liquefaction in less than one cycle, with the soil exhibiting very low resistance to reliquefaction. Throughout all figures presented in this paper, a compression negative sign convention is adopted.

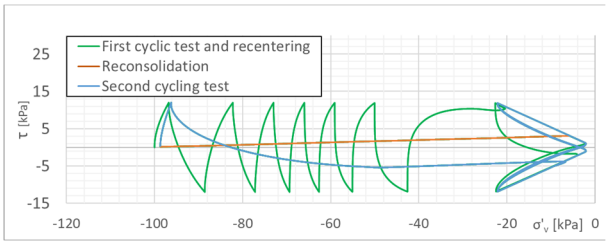

Figure 1. Analysis A.3. $DR_{initial}$ =35 %. CSR = 0.12. $\gamma_{max} \approx 3.0$ % for first cyclic load.

Figure 2 to Figure 5 present the results of the 2nd cyclic loading for 4 of the 44 simulations conducted, each corresponding to a different maximum shear strain value applied during the 1st cyclic loading. All these simulations consider an initial relative density of 35 %.

In the results presented in Figure 2 (which illustrates the same simulation as Figure 1, but showing only the 2nd cyclic loading test), where γ_{max} = 3% during the 1st cyclic loading, liquefaction is reached in less than one cycle for the 2nd cyclic loading. It can be seen that as γ_{max} during the 1st cyclic loading decreases (moving from Figure 2 with a $\gamma_{max} \approx 3\%$ to Figure 5 with a $\gamma_{max} \approx 0.1\%$), the number of cycles required to reach liquefaction during the 2nd cyclic loading increases significantly, peaking at $\gamma_{max} \approx 0.2$ % (Group C).

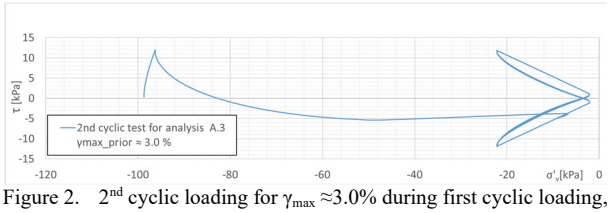

Figure 2. 2nd cyclic loading for $\gamma_{max} \approx 3.0\%$ during first cyclic loading, DR = 35 %. Group A.

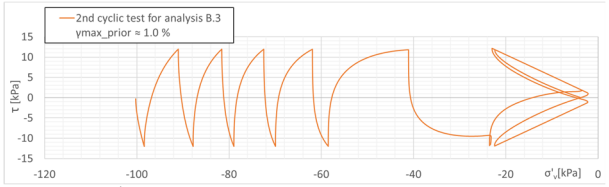

Figure 3. 2nd cyclic loading for $\gamma_{max} \approx 1.0\%$ during first cyclic loading, DR = 35 %. Group B.

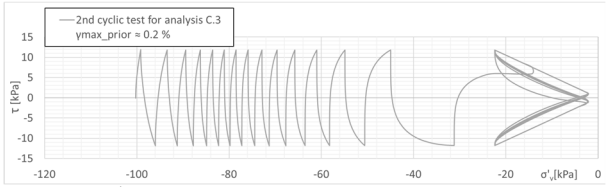

Figure 4. 2nd cyclic loading for $\gamma_{max} \approx 0.2\%$ during first cyclic loading, DR = 35 %. Group C.

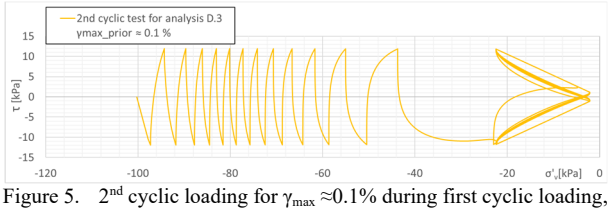

Figure 5. 2nd cyclic loading for $\gamma_{max} \approx 0.1\%$ during first cyclic loading, DR = 35 %. Group D.

Figure 6 to Figure 9 present the results of the 2nd cyclic loading phase for another set of 4 of the 44 simulations conducted with an initial relative density of 72 % and CSR=0.25.

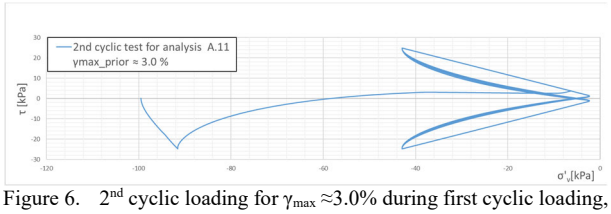

Figure 6. 2nd cyclic loading for γ_{max} ≈3.0% during first cyclic loading, DR = 72 %. Group A.

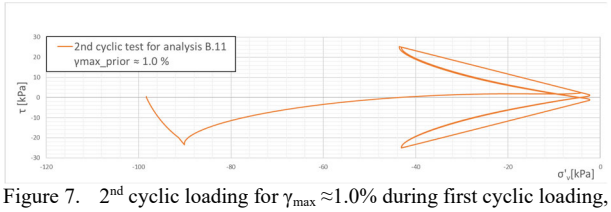

Figure 7. 2nd cyclic loading for γ_{max} ≈1.0% during first cyclic loading, DR = 72 %. Group B.

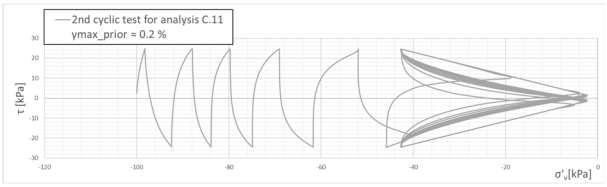

Figure 8. 2nd cyclic loading for γ_{max} ≈0.2% during first cyclic loading, DR = 72 %. Group C.

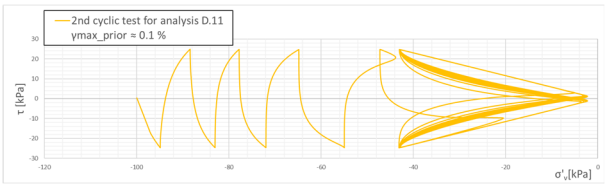

Figure 9. 2nd cyclic loading for γ_{max} ≈0.1% during first cyclic loading, DR = 72 %. Group D.

When comparing the results presented in Figure 2 to Figure 5 (which correspond to a relative density of 35%) with those shown in Figure 6 to Figure 9 (where the relative density is 72%), a similar behaviour can be observed. Specifically, when higher values of the maximum shear strain (γ_{max}) are reached during the 1st cyclic loading (results shown in Figure 2, Figure 6 and Figure 7), the soil experiences a reduction in both stiffness and strength, resulting in liquefaction occurring almost immediately during the 2nd cyclic loading phase.

On the other hand, when lower values of maximum shear strain (γ_{max}) are reached during the 1st cyclic loading phase (results shown in Figure 3 to Figure 4 Figure 5, Figure 8 and Figure 9) the soil's resistance to reliquefaction during the 2nd cyclic loading increases significantly.

Figure 10 summarizes the influence of strain history on reliquefaction resistance, defining liquefaction as the state corresponding to a single amplitude shear strain of 3.0 %.

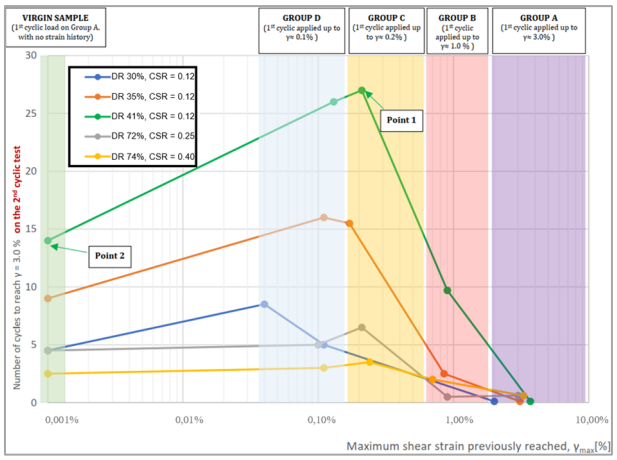

Figure 10. Strain history effect on reliquefaction resistance. Groups A, B, C and D summary.

The vertical axis on Figure 10 corresponds to the number of cycles required to reach γ = 3% on the 2nd cyclic test for all points in the graph, with the exception of the virgin samples Group, which corresponds to the intersection of the curves with the vertical axis. Those simulations (virgin samples) have not experienced any previous shear strain, and therefore the number of cycles in the intersection of the curves with the vertical axis refers to the 1st (and not the 2nd) cyclic test.

For Groups A, B, C, and D, the vertical axis on Figure 10 corresponds to the number of cycles required to achieve a single amplitude shear strain of 3.0 % during the 2nd cyclic loading, as a function of γ_{max} during the 1st cyclic test. In order to clarify the information presented on Figure 10, 2 points of the graph will be explained:

Point 1 (refer to Figure 10): corresponds to the simulation with a DR=41 %, which had been previously tested up to a shear strain of about 0.2 % during the 1st cyclic loading. Later on, the 2nd cyclic loading simulation requires 27 cycles to reach a shear strain of 3.0 % (reliquefaction), which corresponds to an increase in liquefaction resistance when compared with the virgin sample, which required only 14 cycles to reach the same strain level (Point 2).

Point 2 (refer to Figure 10): corresponds to the simulation with a DR=41 % that has not previously experienced any shear strain (virgin sample). After about 14 cycles, it reaches a shear strain of 3.0 % during the 1st cyclic loading.

Figure 10 shows that if the magnitude of the shear strain reached during the 1st cyclic phase reaches values up to around 0.25 % (which includes both Groups C and D), the resistance to reliquefaction for the 2nd cyclic load event increases up to 90 % in terms of the number of cycles required for reaching a single amplitude shear strain of 3.0 %. On the other hand, if the shear strains during the 1st cyclic loading phase reaches values between 0.5 % and 3 % (Groups A and B), the resistance to reliquefaction decreases significantly. Moreover, if a maximum shear strain value of 3.0 % is reached during the 1st cyclic loading phase (Group A), the soil experiences a loss of stiffness and strength resulting in immediate liquefaction during the 2nd loading phase.

While these results do not correspond with the actual experimental behaviour (where the resistance to reliquefaction increases after reaching a shear strain of 3.0 % for all the tests performed by Parra Bastidas (2016)), they do coincide with the behaviour observed in the lab tests performed by Finn et al. (1970) on Ottawa Sand, where a shear strain threshold value above which the resistance to reliquefaction significantly decreases was observed.

Finn et al. (1970) observed that if the shear strains during a previous (or partial) liquefaction exceed that threshold value, the resistance to reliquefaction would decrease. The results obtained in this study show a very similar decrease in reliquefaction resistance, consistent with the findings of Finn et al. (1970), where a reduction in reliquefaction resistance is observed for shear strains above a threshold of 0.5%

It should be noted that all numerical simulations performed in this study adopted a calibration for cyclic direct simple shear (CDSS) tests with no strain history considered. It is possible that a calibration that accounts for reliquefaction through cyclic simple shear tests can reproduce more closely the actual soil behaviour when dealing with reliquefaction.

4 CONCLUSIONS

The single element simulations performed with the constitutive model PM4Sand indicate the existence of a shear strain threshold value, beyond which the resistance to reliquefaction significantly decreases if the threshold values is exceeded in a previous liquefaction event, while the resistance increases if the shear strains remain below that threshold during a previous (or partial) liquefaction event. Despite undergoing reconsolidation, the soil does not regain significant structural resistance, when the critical shear strain threshold (γ_{max}) is exceeded, leading to lasting degradation of the soil fabric. The results support the existence of a shear strain threshold for assessing reliquefaction resistance, which was initially observed in lab tests performed by Finn et al. (1970).

For the examined cases, the results suggest that when the shear strains during a 1st cyclic loading phase fall within the range of [0.03 % - 0.25 %], the resistance to reliquefaction significantly increases for a 2nd event. On the contrary, if the shear strains during a 1st cyclic loading phase lie within the range of [0.5 % - 3.0 %], the reliquefaction resistance for a 2nd liquefaction event significantly decreases.

The presented results provide evidence – obtained through advanced constitutive modelling – of the existence of a shear strain threshold which influences the reliquefaction resistance in sands. These findings support and complement previous experimental studies and provide a basis for enhancing seismic hazard assessment methodologies and developing more reliable geotechnical design criteria for regions with high seismicity.

5 REFERENCES

Boulanger, R.W. & Ziotopoulou, K. 2013. Formulation of a sand plasticity plane-strain model for earthquake engineering applications. Soil Dynamics and Earthquake Engineering, 53, pp.254–267.

Cubrinovski, M., Robinson, K., Taylor, M., Hughes, M. & Orense, R. 2012. Lateral spreading and its impacts in urban areas in the 2010–2011 Christchurch earthquakes. New Zealand Journal of Geology and Geophysics, 55(3), pp.255–269.

Finn, W.D.L., Bransby, P.L. & Pickering, D.J. 1970. Effect of strain history on liquefaction of sand. Journal of the Soil Mechanics and Foundations Division, 96(6), pp.1917–1934.

Ishihara, K. & Okada, S. 1978. Effects of stress history on cyclic behavior of sand. Soils and Foundations, 18(4), pp.31–45.

Nemat-Nasser, S. & Takahashi, K. 1984. Liquefaction and fabric of sand. American Society of Civil Engineers (ASCE).

Nemat-Nasser, S. & Tobita, Y. 1982. Influence of fabric on liquefaction and densification potential of cohesionless sand. Mechanics of Materials, 1(1), pp.43–62.

Parra Bastidas, A.M. 2016. Ottawa F-65 Sand Characterization. ProQuest Dissertations Publishing.

Seed, B., Silver, M.L., Chan, C.K. & Lee, K.L. 1977. Influence of seismic history on liquefaction of sands. Journal of the Geotechnical Engineering Division, 103(GT4), pp.257–270.

Suzuki, T. & Suzuki, T. 1988. Effects of density and fabric change on reliquefaction resistance of saturated sand. Soils and Foundations, 28(2), pp.187–195.

Van Ballegooy, S., Malan, P., Lacrosse, V., Jacka, M.E., Cubrinovski, M., Bray, J.D., O'Rourke, T.D., Crawford, S.A. & Cowan, H. 2014. Assessment of liquefaction-induced land damage for residential Christchurch. Earthquake Spectra, 30(1), pp.31–55.

Verdugo, R. & González, J. 2015. Liquefaction-induced ground damages during the 2010 Chile earthquake. Soil Dynamics and Earthquake Engineering, 79, pp.280–295.

Yamada, S., Sasaki, Y., Nozu, A., Suzuki, T. & Yasuda, S. 2010. Effects on reliquefaction resistance produced by changes in anisotropy during liquefaction. Tokyo: Japanese Geotechnical Society.

Yasuda, S. & Tohno, I. 1988. Sites of reliquefaction caused by the 1983 Nihonkai-Chubu earthquake. Tokyo: Japanese Geotechnical Society.